

# Alternative Methods to Calculate Electromagnetic Transients in Grounding Systems

Jaimis S. L. Colqui;  
Anderson R. J. de Araújo;  
Sérgio Kurokawa  
Dept. of Electrical Engineering  
São Paulo State University  
Ilha Solteira, Brazil  
jeimis.leon@gmail.com  
anderjusto@yahoo.com.br  
kurokawa@dee.feis.unesp.br

Claudiner M. Seixas  
Federal Institute of São Paulo  
Votuporanga, São Paulo, Brazil  
claudiner@ifsp.edu.br

**Abstract**—Grounding electrodes are essential in electrical power system to maintain a reliable operation, and to guarantee the safety of personnel and equipment. When a lightning strikes at a transmission tower, surge current waves travel to the foundations of the structure which are partially absorbed by the grounding impedance. As a consequence, the electrical potential increases in relation to a remote reference, which is named Grounding Potential Rising (GPR). These curves are very important to verify if the step voltages are in accordance with specific standards to guarantee a safety conditions during the transient state. In this paper, impedance of some grounding systems are calculated by classic models for a large frequency range, varying in different lengths and buried in homogeneous soils. Then, the GPR curves are by two recursive methods directly in time domain. These methods applies Vector Fitting technique on each grounding impedance response, where the poles and residues are obtained. Then, employing the recursive convolution and trapezoidal method, the GPR are computed directly in time domain. These curves are compared with the classic Numerical Laplace Transform (NLT) which have shown a good agreement with the recursive methods.

**Index Terms**—grounding electrodes, recursive methods, lightning, electromagnetic transients

## I. INTRODUCTION

Grounding electrodes have many functions in electrical power systems, such as: (a) to provide a low impedance for ground fault currents into soil; (b) to minimize the probability of backflashovers in transmission towers hit by lightning; (c) to decrease step voltages to protect living being around to transmission towers and (d) to establish a reference potential for all equipment connect to the electrical system [1], [2].

In this context, grounding impedance has been calculated by either analytical modeling or numerical methods as proposed

This study was financed by the Coordenação de Aperfeiçoamento de Pessoal de Nível Superior - Brasil (CAPES) -Finance Code 001 and by the São Paulo Research Foundation (FAPESP), grant: 2014/18551-6

by several researchers in the technical literature. One of the most employed models for representing simple electrodes is the Transmission Line Model. In this model, the vertical or horizontal electrodes are seen as a short transmission line, whose parameters are distributed per-unit length, assuming quasi-static assumption [1], [2]. On the other hand, numerical methods are also employed to computed grounding impedance of complex electrode arrangements such as counterpoise electrodes and grounding grids. These methods are based on electromagnetic field theory, which they solve the Maxwell equations. Such numerical methods employed are: Method of Moments (MoM) [3], [4]; Finite Difference Time Domain (FDTD) [5], [6], including no-linear effects in the soil; Finite Element Method (FEM) [7] and by (iv) hybrid methods, combining electromagnetic field theory with electric circuit approach [8], [9].

When lightning strikes at the transmission tower, a surge current travels to the base foundations where is partially dissipated through the grounding system and the other parcel is reflected back to the tower top [10]. In the grounding electrodes, a electrical potential raises up the reference voltage which can damage equipment and affect the safety of the personnel. This electrical potential rising is named Grounding Potential Rising (GPR), and it is defined as the product of the grounding electrode impedance, in relation to a remote earth, and the current that flows through that electrode impedance. The value of GPR is a important parameter to verify if the step voltages are in accordance with specific standards for grounding systems as defined in [11]. One way to reduce the GPR is to increase the electrode length for cylindrical conductors or the area of the grounding grids.

Some methods calculate the grounding impedance in a large frequency range, as well as for the spectrum of the lightning current injected at the grounding system. The GPR is calculate by taking the Numerical Laplace Transform of the product

of grounding impedance and current. Furthermore, recursive methods can be an alternative to compute GPR directly in time domain. In these methods, the Vector Fitting (VF) is used to fit grounding impedance curves into a rational function. Then, poles and residues obtained from the fitting technique are employed in the recursive methods, as presented further in this article. In these methods, there is no need of Inverse Laplace Transform or Electromagnetic Transient Programs (EMTP)-type simulation tools, to compute GPR curves directly in time domain.

In this paper, grounding impedances of several electrodes buried in homogeneous soils are calculated by analytical modelling and numerical methods. Then, two recursive methods are presented to compute the GPR curves of each grounding system directly in time domain. These curves are compared with the classic Numerical Laplace Transform (NLT), which is considered the reference response. Transient GPR responses are in a good agreement with those computed by NLT.

The paper is organized as follows: In Section II, the TLM and HEM models to calculate the grounding impedance are described. In section III, the Vector Fitting technique, recursive convolution and trapezoidal method applied in state-space equations are presented. In section IV, the two recursive methods to compute GPR are described. In section V, grounding impedance of several electrodes systems buried in homogeneous soils are computed by TLM and HEM. The GPR curves are calculated by NLT,  $PM_1$  and  $PM_2$ . Finally, conclusions are presented in Section VI.

## II. GROUNDING SYSTEM MODELLING

In this paper, two different methods are employed to calculate the impedance of the grounding systems in the frequency domain, as following:

### A. Transmission Line Modelling

A cylindrical electrode either buried vertically or horizontally in a ground can be modeled as a short transmission line, using the Transmission Line Model (TLM). In TLM, electrical parameters of the electrode are distributed along its length, in per-unit-length (p.u.l.), and the currents and voltage are computed by the hyperbolic equations. For estimating the grounding impedance, its receiving end is left open. In Fig. 1, it is depicted a generic horizontal electrode of length  $d$  which is buried in a soil of resistivity  $\rho$ , relative permeability  $\mu_r$  and relative permittivity  $\epsilon_r$ . In Fig. 1, **A** and **B** are, respectively, the sending and receiving end of this short transmission line. The current  $I_A(s)$  and voltage  $V_A(s)$ , as a function of the current  $I_B(s)$  and voltage  $V_B(s)$  at the receiving end, are calculated in the frequency domain by (1):

$$\begin{bmatrix} V_A(s) \\ I_A(s) \end{bmatrix} = \begin{bmatrix} A & B \\ C & D \end{bmatrix} \begin{bmatrix} V_B(s) \\ I_B(s) \end{bmatrix} \quad (1)$$

where the elements A, B, C and D are given as below

$$A = \cosh(\gamma(s)d) \quad (2a)$$

$$B = Z_c(s) \sinh(\gamma(s)d) \quad (2b)$$

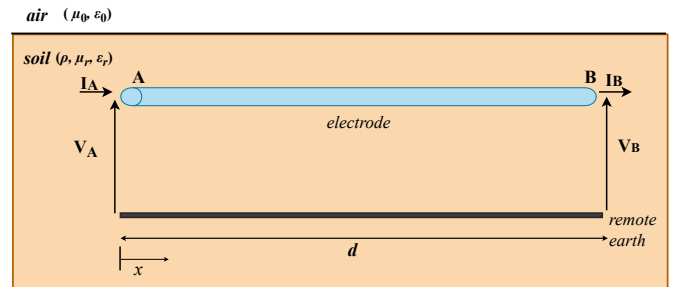


Fig. 1: Horizontal electrode seen as a short transmission line.

$$C = \frac{1}{Z_c(s)} \sinh(\gamma(s)d) \quad (2c)$$

$$D = \cosh(\gamma(s)d) \quad (2d)$$

The variables  $\gamma(\omega)$  [m<sup>-1</sup>] and  $Z_C(\omega)$  [ $\Omega$ ] are the propagation function and the characteristic impedance of a transmission line, respectively, and they are given by (3) and (4)

$$\gamma(s) = \sqrt{(R + sL)(G + sC)} \quad (3)$$

$$Z_C(s) = \sqrt{\frac{R + sL}{G + sC}} \quad (4)$$

Where  $s = j\omega$  [rad.s<sup>-1</sup>] is the complex frequency,  $\omega = 2\pi f$  [rad.s<sup>-1</sup>] is the angular frequency, and  $f$  is the frequency [Hz]. The parameter  $R$  [ $\Omega/m$ ] and  $L$  [H/m] represent the p.u.l. longitudinal resistance and inductance of the grounding electrode buried in the soil, respectively. The parameters  $G$  [S/m] and  $C$  [F/m] represent the p.u.l. transversal conductance and capacitance of the electrode, respectively. In frequency domain, considering that the horizontal (or vertical) electrode is an open circuit at the end B ( $x = d$ ,  $I_B(s) = 0$ ), the grounding impedance  $Z_{gr}$  can be calculated by [3], [12]:

$$Z_{gr}(s) = Z_C \coth(\gamma(s)d) \quad (5)$$

Many authors have proposed different distributed parameter approaches for representing grounding electrodes in the literature [3], [12]–[15]. Based on Fig. 1, for the horizontal electrode, the series resistance  $R_h$  and inductance  $L_h$  and shunt conductance  $C_h$  and capacitance  $G_h$  parameters are defined by [14]:

$$R_h = \frac{\rho_c}{\pi a^2} \quad (6a)$$

$$L_h = \frac{\mu}{2\pi} \left[ \ln \left( \frac{2d_h}{\sqrt{2ha}} \right) - 1 \right] \quad (6b)$$

$$G_h = \frac{\pi}{\rho} \left[ \ln \left( \frac{2d_h}{\sqrt{2ha}} \right) - 1 \right]^{-1} \quad (6c)$$

$$C_h = \pi \epsilon_0 \epsilon_r \left[ \ln \left( \frac{2d_h}{\sqrt{2ha}} \right) - 1 \right]^{-1} \quad (6d)$$

For the vertical grounding electrode, the series resistance  $R_v$  and inductance  $L_v$  and shunt conductance  $G_v$  and capacitance  $C_v$  are defined by [13]:

$$R_v = \frac{\rho_c}{\pi a^2} \quad (7a)$$

$$L_v = \frac{\mu}{2\pi} \left[ \ln \left( \frac{2d_v}{a} \right) - 1 \right] \quad (7b)$$

$$G_v = \frac{2\pi}{\rho} \left[ \ln \left( \frac{4d_v}{a} \right) - 1 \right]^{-1} \quad (7c)$$

$$C_v = 2\pi\epsilon_0\epsilon_r \left[ \ln \left( \frac{4d_v}{a} \right) - 1 \right]^{-1} \quad (7d)$$

Equations (6) to (7),  $\mu_r$  is the permeability of the conductor,  $\epsilon_r$  is the relative permittivity of the soil while  $d_h$  and  $d_v$  are the horizontal and vertical electrode lengths and  $a$  is the electrode radius. A vertical or horizontal electrode can be represented by its distributed parameter (p.u.l.) when each segment of the electrode ( $\Delta l$ ) is much smaller than one tenth of the wavelength ( $\lambda$ ) of the injected current [1], [16].

### B. Hybrid Electromagnetic Model

A hybrid model has been employed to compute the grounding impedances of complex grounding systems, such as counterpoise electrodes and grounding grids. This model combines numerical Method of Moments (MoM), to solve electromagnetic theory applied to the electrodes, with electric circuit representation, which is named Hybrid Electromagnetic Model (HEM) [9], [17]. In HEM, the electrode is divided in small segments which generates electromagnetic fields due to transversal and longitudinal current through the conductor. The transversal current is related to rising in the electrical potential while the longitudinal current is related to the voltage difference along the conductor itself. In this paper, the grounding impedance of counterpoise electrodes and grids are calculated for a large frequency range where MoM is applied to solve the integral field equations.

Counterpoise electrodes are typically used as footing grounding conductors running along the transmission line axis. In this case, 4-long grounding electrodes are employed to produce a low grounding impedance where the length of each conductor depends on the soil resistivity as presented in Table 3 of [18]. There are no analytical formulas to compute the grounding impedance of the counterpoise electrodes in frequency domain. Then, the numerical methods are employed to assess grounding impedance of counterpoise electrodes for in different arrangements and soils, as further presented.

### III. RECURSIVE METHODS

The recursive methods can be employed to compute GPR. In these methods, the impedance response of any grounding system, in frequency domain, is fitted by Vector Fitting technique, where a rational function is obtained based on the poles and residues of original curve. In this section, the VF technique is briefly presented, and two recursive methods  $PM_1$  and  $PM_2$

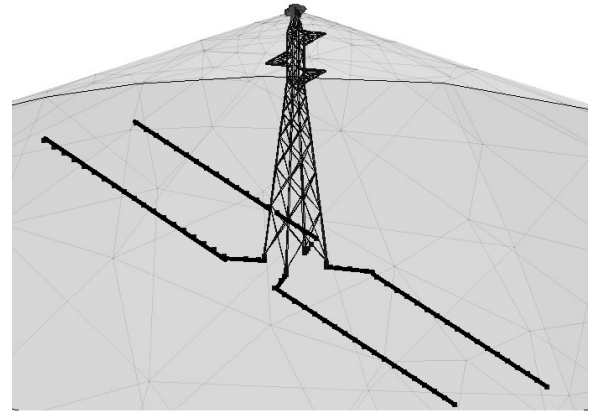


Fig. 2: Generic counterpoise electrodes as grounding system in transmission towers.

are described.  $PM_1$  is a recursive convolution method and  $PM_2$  is based on trapezoidal method associated to a state-space representation.

For computing GPR curves directly in time domain, the rational function  $F(s)$  can be interpreted as the  $Z_{gr}(s)$  in frequency domain is which is multiplied by the current applied at the sending terminal of the electrode.

$$V_k(s) = F(s)I_k(s) \quad (8)$$

where rational function  $F(s)$  represents the impedance of any grounding impedance in the frequency domain.

#### A. Vector Fitting technique

The transfer functions  $F(s)$  are approximated by employing a functions fitting technique applied in each frequency response. The technique used in this article is Vector Fitting (VF), where a rational function  $F(s)$  is approximated for each frequency response curve. This approximation  $F(s)$ , in the frequency domain, is obtained by a polynomial function, as given by [19]

$$F(s) = \frac{z_0 + z_1s + z_2s^2 + \dots + z_{n-1}s^{n-1}}{p_0 + p_1s + p_2s^2 + \dots + p_ns^n} \quad (9)$$

Where the complex angular frequency is given by  $s = j\omega$ . The VF technique considers that a rational function can be expanded as a finite sum of  $n$  rational functions described by its general form (10) [19].

$$F(s) \simeq \sum_{j=1}^n \left( \frac{z_j}{s + p_j} \right) \quad (10)$$

where  $z_j$  are the residues and  $p_j$  are the poles of the rational approximation of generic function  $F(s)$ . The fitted function in (10) transformed to the time domain is a sum of exponential functions as given by (11).

$$f(t) = \sum_{j=1}^n (z_j e^{-p_j t}) \quad (11)$$

The advantage of this process is that exponential functions are easily used directly in the recursive convolution method, as shown in the following section.

### B. Recursive convolution method PM<sub>1</sub>

To determine an analytical solution of GPR in (8) need to be transformed from the frequency domain to the time domain. To achieve this outcome, the definition of the convolution integral [20], as shown in (12), is employed.

$$v_k(t) = f(t) * i_k(t) = \int_{-\infty}^{+\infty} f(\tau) i_k(t - \tau) d\tau \quad (12)$$

The evaluation of the convolution in (12) in discrete time is computationally expensive. However, using the rational function approximation in  $F(s)$ , an efficient recursive convolution method can be applied, and integral (12) can be rewritten as a sum of exponential functions, as shown in (13) [19].

$$v_k(t) = \int_{\tau}^{+\infty} \sum_{j=1}^n [z_j e^{-p_j t} i_k(t - \tau)] d\tau \quad (13)$$

where  $z_j$  and  $p_j$  are the residues and poles of the approximation of the rational functions  $F(s)$ . The analytical solution of the vector  $v_k(t)$  is determined recursively from  $v_k(t - \Delta t)$  by

$$v_k(t) = \alpha_1 v_k(t - \Delta t) + \beta_1 i_k(t) + \mu_1 i_k(t - \Delta t) \quad (14)$$

where coefficients  $\alpha_1$ ,  $\beta_1$  and  $\mu_1$  are derived based on the assumption that  $i_k(t)$  is linear in the small time-step  $\Delta t$ , and the coefficients are given by:

$$\alpha_1 = \sum_{j=1}^n e^{-p_j \Delta t} \quad (15a)$$

$$\beta_1 = \sum_{j=1}^n \frac{z_j}{p_j} \left( 1 - \frac{1}{p_j \Delta t} (1 - e^{-p_j \Delta t}) \right) \quad (15b)$$

$$\mu_1 = \sum_{j=1}^n \frac{z_j}{p_j} \left( e^{-p_j \Delta t} + \frac{1}{p_j \Delta t} (1 - e^{-p_j \Delta t}) \right) \quad (15c)$$

Where the  $v_k(t)$  is the GPR curve in time domain.

### C. Recursive trapezoidal rule PM<sub>2</sub>

Another method to compute GPR directly in time domain is the recursive trapezoidal rule which is associated to state-space equations. First, replacing (10) in (8), the voltage  $V_k(s)$  yields

$$V_k(s) = \sum_{j=1}^n \left( \frac{z_j}{s + p_j} \right) I_k(s) \quad (16)$$

From (16) introduced a generic variable  $X_j(s)$ , for all  $1 \leq j \leq n$ , which it can be express as:

$$X_j(s) = \frac{z_j}{s + p_j} I_k(s) \quad (17)$$

Applying the Inverse Laplace Transform in (17), the state-space equation for the  $j$ -th element of  $X_j$  is expressed by:

$$\begin{aligned} \frac{dx_j(t)}{dt} &= A_j x_j(t) + B_j i_k(t) \\ v_{k,j}(t) &= C_j x_j(t) + D_j i_k(t) \end{aligned} \quad (18)$$

In (18)  $v_{k,j}(t)$  and  $x_j(t)$  are the Laplace Transform of  $V_{k,j}(s)$  and  $X_j(s)$ , respectively. The terms  $v_{k,j}(t)$  represent the voltage no terminal  $k$  do  $j$ -th element, and  $x_j(t)$  is the state introduced. The parameters  $A_j$ ,  $B_j$ ,  $C_j$  e  $D_j$  are defined by

$$A_j = -p_j, \quad B_j = z_j, \quad C_j = 1, \quad D_j = 0 \quad (19)$$

where  $z_j$  and  $p_j$  are the residues and poles of the approximation of the rational functions  $F(s)$ . The analytical solution of the linear system in (18) is determined for the trapezoidal rule (Heuns method):

$$v_k(t) = \alpha_2 v_k(t - \Delta t) + \beta_2 i_k(t) + \mu_2 i_k(t - \Delta t) \quad (20)$$

where coefficients  $\alpha_2$ ,  $\beta_2$  and  $\mu_2$  are constant coefficients and defined by

$$\alpha_2 = \sum_{j=1}^n \left( 1 + \frac{p_j \Delta t}{2} \right)^{-1} \left( 1 - \frac{p_j \Delta t}{2} \right) \quad (21a)$$

$$\beta_2 = \sum_{j=1}^n \left( 1 + \frac{p_j \Delta t}{2} \right)^{-1} \left( \frac{z_j \Delta t}{2} \right) \quad (21b)$$

$$\mu_2 = \sum_{j=1}^n \left( 1 + \frac{p_j \Delta t}{2} \right)^{-1} \left( \frac{z_j \Delta t}{2} \right) \quad (21c)$$

Where the  $v_k(t)$  is the GPR. All the three methods employed to calculate GPR are summarized in the next section.

## IV. METHODOLOGY

The three methods employed to calculate the GPR curves are presented, and summarized, in Fig. 3.

In Fig. 3-a, the classical NLT is employed to compute the GPR. In this method, the grounding impedance  $Z_{gr}(s)$  is computed, either by TLM or HEM, in a large frequency range and the impulsive current spectrum  $I(s)$  is calculated in frequency domain. Then, the both curves are multiplied and GPR is computed by applying the inverse Numerical Laplace Transform. In Fig. 3-(b), the recursive method-1 ( $PM_1$ ) computes the  $Z_{gr}(s)$  by TLM or HEM and then, the VF technique is applied in each frequency response curve. The residues  $r_j$  and poles  $z_j$  are obtained and the impulsive current  $I_k(t)$  is represented by a double-exponential function in time domain and GPR curve are computed by recursive convolutions given by (13) and (14). The method ( $PM_2$ ), also applies the VF technique in each  $Z_{gr}(s)$  response. Then, the state-space representation is used and GPR curves are computed by Method of Heun in time domain, as described by (18) and (20).

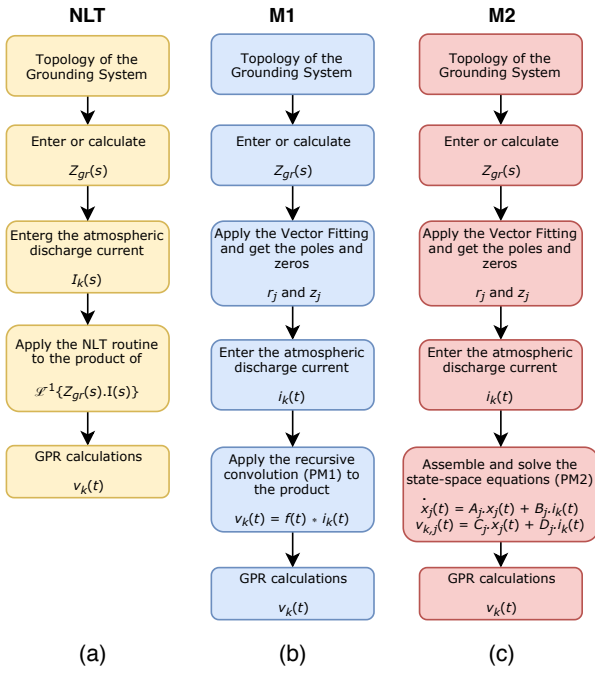


Fig. 3: Steps of each method: (a) NLT; (b)  $PM_1$  and (c)  $PM_2$ .

## V. NUMERICAL RESULTS

The numerical results are divided in two sections. In section V-A, the grounding impedance of vertical and horizontal electrodes are calculated by TLM while the impedance of counterpoise electrodes are calculated by HEM. In the section V-B, the GPR for each topology is calculated by NLT,  $PM_1$  and  $PM_2$ . The frequency dependence on the soil parameters and ionization effect are not considered in these simulations.

### A. Grounding Impedance of electrodes

Grounding impedances of vertical and horizontal electrodes are calculated by the TLM as a function of a frequency range for different soil resistivities. Fig. 4 depicts the horizontal and vertical electrodes buried in a generic soil of relative permeability  $\mu_r$ , relative permeability  $\epsilon_r$  and soil resistivity  $\rho$ . The geometrical parameters of these electrodes are: lengths  $d_h = d_v = 1$  m, burial depth  $h = 1$  m and radius  $a = 12.5$  mm. The top of the vertical electrode is on the surface air/soil. The electrical parameters of the soil are:  $\mu_r = 1$ ,  $\epsilon_r = 10$  and  $\rho$  of 100, 500 and 1,000  $\Omega\text{m}$ . The electrodes are made of copper  $\rho_c = 1.724 \times 10^{-8} \Omega\text{m}$ .

In Figs. 5 and 6 depicted the grounding impedance of horizontal and vertical electrodes. It may be noted that the magnitude of the grounding impedance of horizontal and vertical electrodes present a resistive behaviour at low frequencies (below 1 MHz). In this case, the magnitude of this resistance depends on the ground which is higher as the soil resistivity increases. After a switching frequency, the grounding impedance may assume a inductive or capacitive behaviour which is strongly affect by the frequency range. The magnitudes of the grounding impedance for horizontal

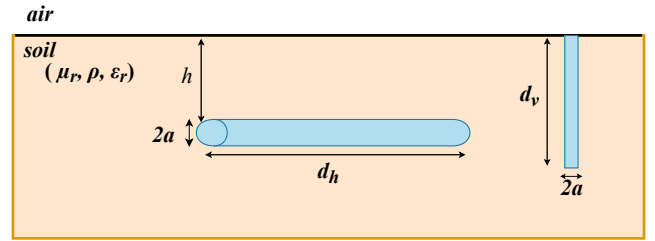
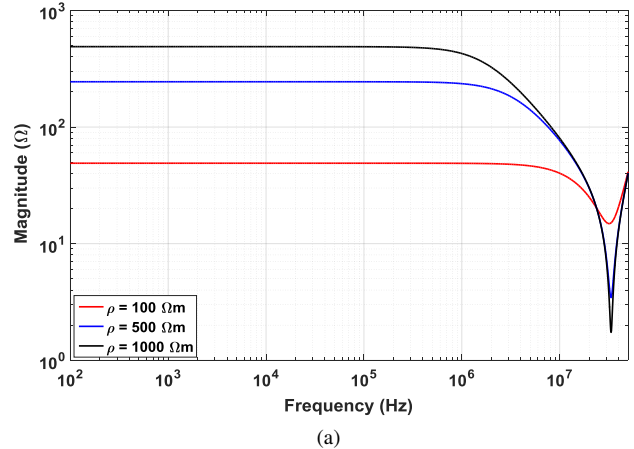
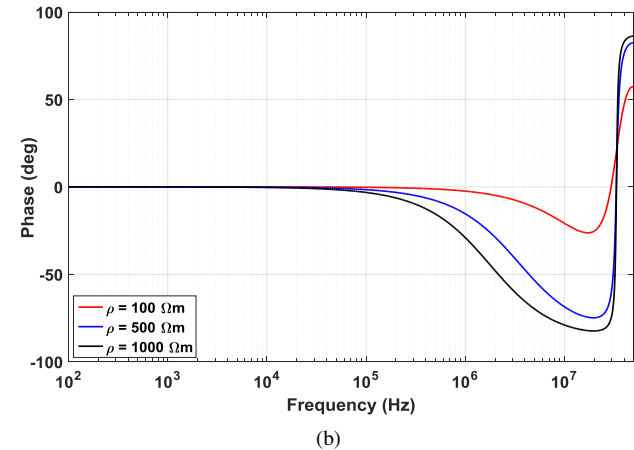


Fig. 4: Horizontal and vertical electrodes in a generic soil.



(a)

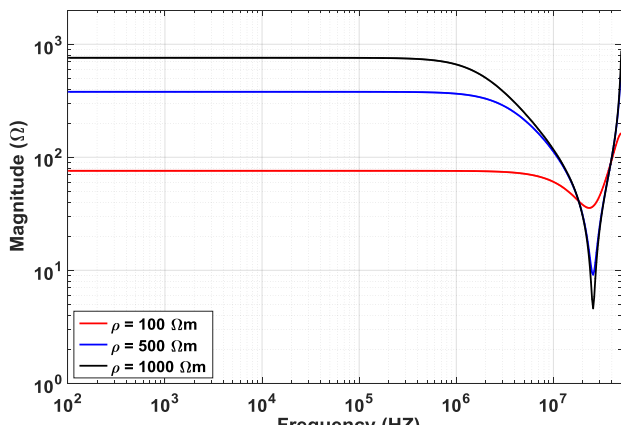


(b)

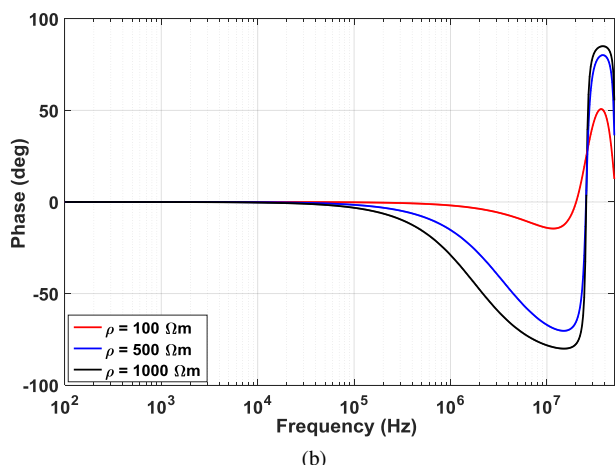
Fig. 5: Grounding impedances of a 1-m horizontal electrode for different soil resistivities [ (a) Magnitude and (b) phase.]

electrode are lower than the vertical electrode. As given by Figs. 5 and 6, at low frequencies, the magnitude of impedance for the horizontal electrode are 50, 150 and 500  $\Omega$  for the soils of 100, 500 and 1,000  $\Omega\text{m}$ , respectively. For the vertical electrode, these values are approximately of 75, 400 and 800  $\Omega$  for the same sequence of resistivity. At low frequencies, the conductance  $G_v$  is higher than  $G_h$  which predominates the resistive behaviour of grounding impedance of the vertical electrode over the horizontal electrode.

Fig. 7 depicts the counterpoise electrodes where  $d$  is distance between tower-feet  $L_1$  is the total length of the electrode and  $a$  is the conductor radius,  $h_1$  is the thickness of the soil



(a)



(b)

Fig. 6: Grounding impedance of a 1-m vertical electrode for different soil resistivities [(a) Magnitude and (b) phase.]

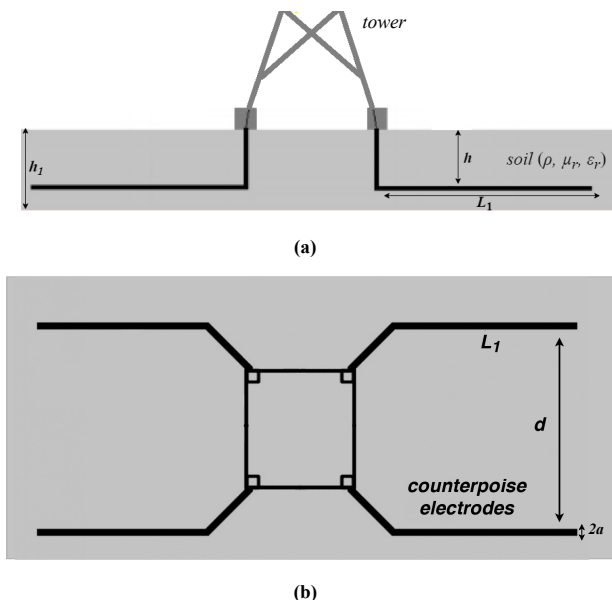
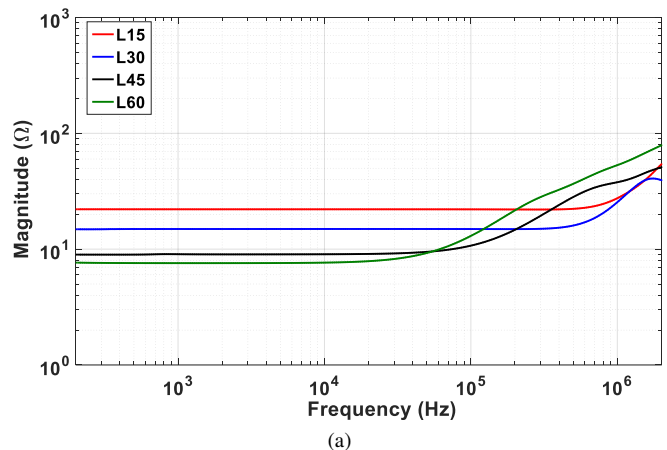
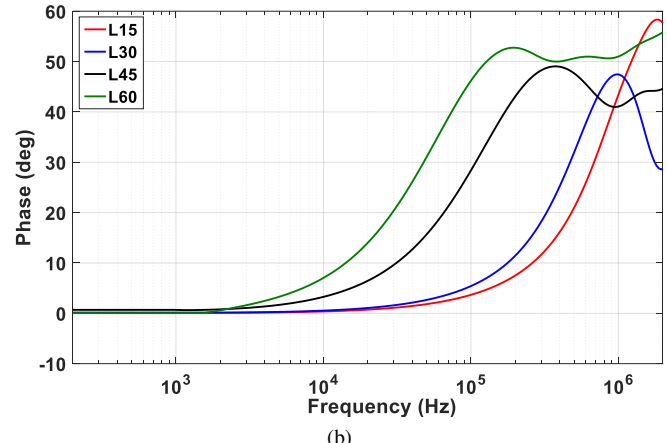


Fig. 7: Counterpoise electrodes:[(a) Side view and (b)Top view].



(a)



(b)

Fig. 8: Grounding impedance of the counterpoise electrodes for different lengths  $L_1$  [(a) Magnitude and (b) phase.]

layer and  $h$  is the burial depth. The values of geometrical parameters are:  $h = 0.50$  m,  $h_1 = 10$  m,  $d = 3$  m,  $a = 12.5$  mm. The soil parameters are:  $\rho = 1,000 \Omega\text{m}$ ,  $\mu_r = 1$ ,  $\epsilon_r = 10$ ; The impedance of the counterpoise is computed for 4 different lengths  $L_1 = 15, 30, 45$  and  $60$  m. The grounding impedance for different length is depicted in Fig. 8.

At low frequencies, a resistive behaviour is observed, however the frequency range where the resistance is constant depends on the electrode length  $L_1$ . After a switching frequency, the impedances of the counterpoise electrodes present predominately inductive behaviour. The larger electrode length  $L_1$  is, the lower is the magnitude of the resistance at low frequencies and also more inductive.

#### B. GPR calculation employing recursive methods

The GPR curves for each topology are computed by NLT,  $PM_1$  and  $PM_2$ . The lightning is modelled by a impulsive source current given by a double exponential function injected at the top of vertical, horizontal electrodes and at the center of counterpoise electrodes.

The current injected is described as:  $i_k(t) = I_0(e^{-\alpha t} - e^{-\beta t})$ , where  $I_0 = 1.037$  kA,  $\alpha = 1.47 \times 10^4 \text{s}^{-1}$  and  $\beta =$

$2.47 \times 10^6 \text{ s}^{-1}$  ( 1.20/50  $\mu\text{s}$  exponential curve).

Initially, for the vertical and horizontal electrodes, the GPR curves are presented in Figs. 9 and 10, where  $d_h = d_v = 1 \text{ m}$ . The GPR curves are strongly dependent on the soil resistivity, where the higher soil resistivity results in a higher GPR peaks. The peaks for the horizontal electrodes are, approximately, 50 kV, 245 kV and 490 kV while for the vertical electrode is 75 kV, 380 kV and 760 kV for soil of 100, 500 and 1,000  $\Omega\text{m}$  respectively. Comparing the GPR curves, it may be noted that GPR peaks of horizontal electrode are lower than the vertical electrode for a fixes soil.

The GPR curves for the counterpoise electrodes are presented in Fig. 11 for a fixed soil resistivity of 1,000  $\Omega\text{m}$ . As expected, the wave-shape of the GPR depends on electrode length where the lower peaks are obtained when the larger conductors are employed. The GPR peaks for counterpoise electrodes of length 15, 30, 45 and 60 m are 30 kV, 22 kV, 15 kV and 6.80 kV respectively. In comparison to the GPR curves of cylindrical electrodes (horizontal  $GPR_{peak} = 480 \text{ kV}$ , and vertical  $GPR_{peak} = 760 \text{ kV}$ ), for soil of  $\rho = 1,000 \Omega\text{m}$ , a significant reduction is obtained for the counterpoise electrodes. Figs. (9) to (11) shows that the recursive methods  $PM_1$  and  $PM_2$  have proved to be very accurate in comparison to the NLT, where all the curves present a good agreement.  $PM_1$  and  $PM_2$  compute GPR curves directly in time domain and they do not require inverse Laplace/Fourier transform. Additionally, once the generic poles and residues are calculated by VF technique,  $PM_1$  and  $PM_2$  will compute the transient response by simple recursive convolution or trapezoidal methods. It is not necessary to implement any electric circuit for each grounding impedance curve in (EMTP)-type simulation tools, to calculate the transient response as proposed by [17].

## VI. CONCLUSIONS

This paper has presented the impedance for different grounding systems in homogeneous soil calculated by TLM and HEM over a large frequency range. It is shown the magnitude of the grounding impedances depend on the geometrical parameters, arrangement of the conductors and soil resistivity. At low frequencies, all grounding systems present a resistivity behaviour constant for a large frequency range. Above a switching frequency, grounding impedance may assume inductive or capacitive behaviour at high frequencies. The wave-shapes of the GPR, especially the peak, are strongly affected by the soil resistivity, electrode arrangement and length.

The methods  $PM_1$  and  $PM_2$  have been presented to compute the GPR curves directly in time domain. The GPR curves were computed for different grounding systems when they are hit by a lightning strike, modelled as a double-exponential function. The  $PM_1$  and  $PM_2$  are based on the poles and residues from the fitting technique of the grounding impedance curves. It may be seen that the recursive methods are in a good agreement with the NLT response. The proposed

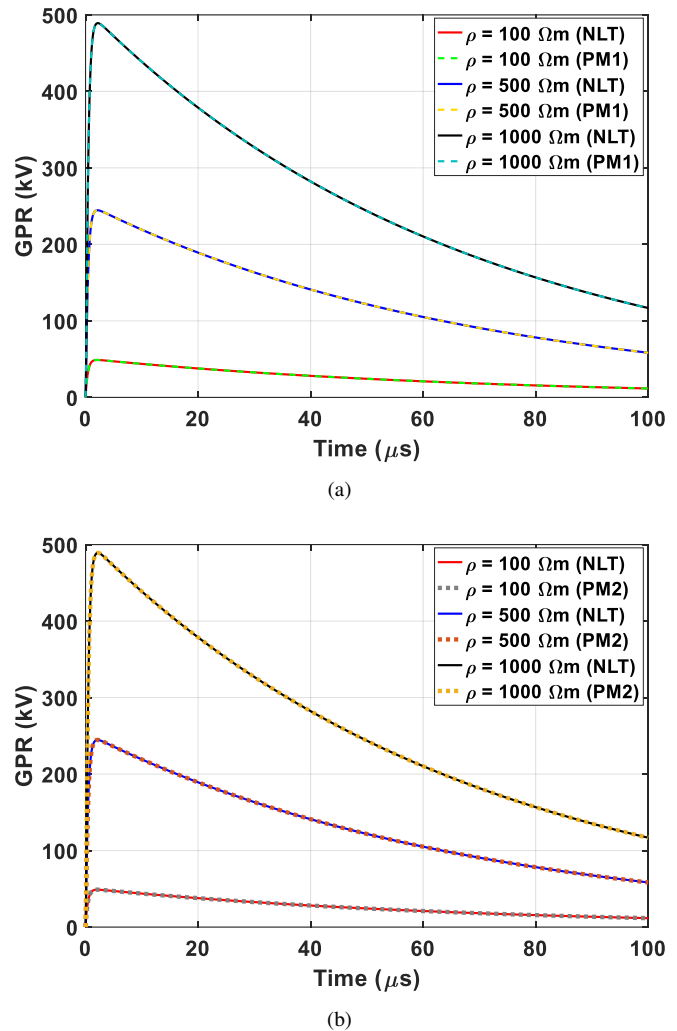
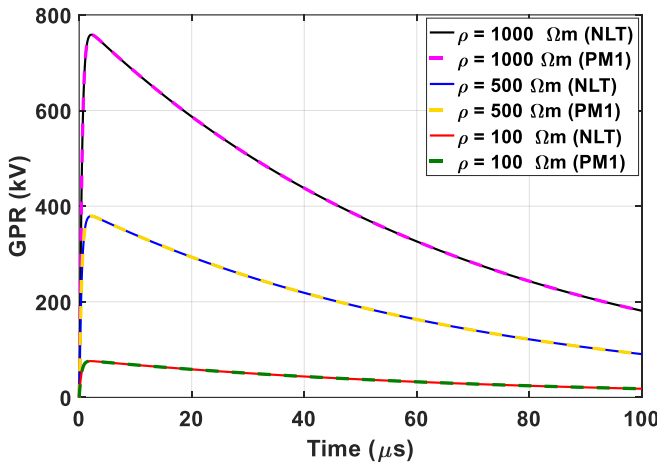
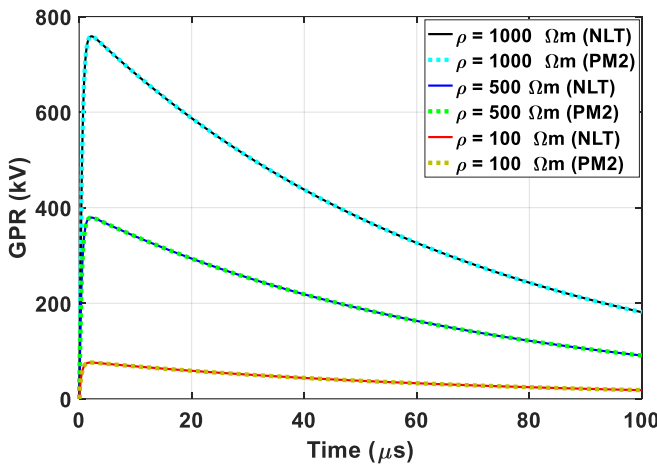


Fig. 9: GPR curves of a 1-m horizontal electrode for several soil resistivities obtained by: [(a) NLT and  $PM_1$ ; (b) NLT and  $PM_2$  ].

methods provide transient response directly in time domain, do not require any inverse Laplace Transform nor need equivalent electric circuit representation in (EMTP)-type simulation tools for the transient analysis .

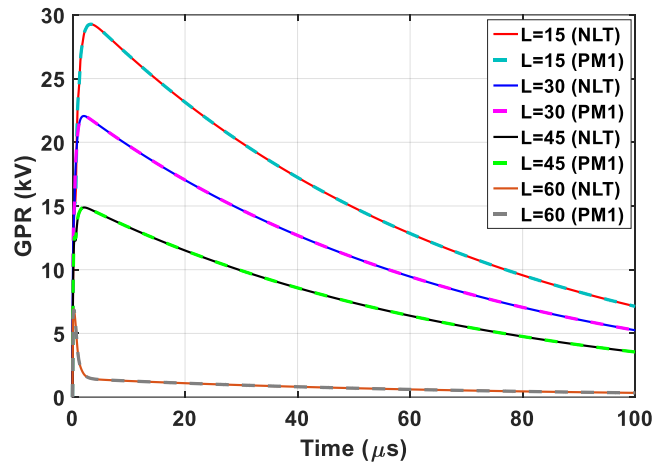


(a)

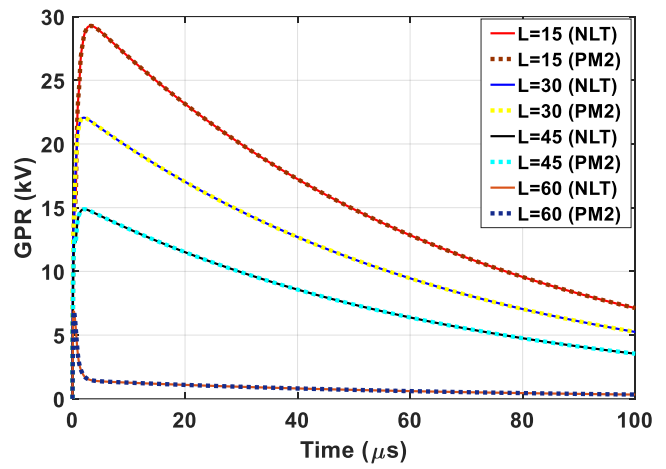


(b)

Fig. 10: GPR curves of a 1-m vertical electrode for several soil resistivities obtained by: [(a) NLT and PM<sub>1</sub>; (b) NLT and PM<sub>2</sub> ].



(a)



(b)

Fig. 11: GPR curves of the counterpoise electrodes buried in a soil of  $\rho = 1,000 \Omega\text{m}$  for several lengths  $L_1$  obtained by: [(a) NLT and PM<sub>1</sub>; (b) NLT and PM<sub>2</sub> ].

## REFERENCES

- [1] S. Chiheb, O. Kherif, M. Teguar, A. Mekhaldi, and N. Harid, "Transient behaviour of grounding electrodes in uniform and in vertically stratified soil using state space representation," *IET Science, Measurement Technology*, vol. 12, no. 4, pp. 427–435, 2018.
- [2] O. Kherif, S. Chiheb, M. Teguar, A. Mekhaldi, and N. Harid, "Time-domain modeling of grounding systems impulse response incorporating nonlinear and frequency-dependent aspects," *IEEE Transactions on Electromagnetic Compatibility*, vol. 60, no. 4, pp. 907–916, Aug 2018.
- [3] L. Grcev, "Modeling of grounding electrodes under lightning currents," *IEEE Transactions on Electromagnetic Compatibility*, vol. 51, no. 3 PART 1, pp. 559–571, 2009.
- [4] S. Fortin, Y. Yang, J. Ma, and F. P. Dawalibi, "Electromagnetic fields of energized conductors in multilayer soils," in *Proceedings - Fourth Asia-Pacific Conference on Environmental Electromagnetics, CEEM'2006*, 2006, pp. 893–899.
- [5] Y. Baba, N. Nagaoka, and A. Ametani, "Modeling of thin wires in a lossy medium for FDTD simulations," *IEEE Transactions on Electromagnetic Compatibility*, vol. 47, no. 1, pp. 54–60, 2005.
- [6] M. Tsumura, Y. Baba, N. Nagaoka, and A. Ametani, "FDTD simulation of a horizontal grounding electrode and modeling of its equivalent circuit," *IEEE Transactions on Electromagnetic Compatibility*, vol. 48, no. 4, pp. 817–824, 2006.
- [7] Y. Liu, N. Theethayi, and R. Thottappillil, "An engineering model for transient analysis of grounding system under lightning strikes: Nonuniform transmission-line approach," *IEEE Transactions on Power Delivery*, vol. 20, no. 2 I, pp. 722–730, 2005.
- [8] R. Araneo, M. Maccioni, S. Lauria, A. Geri, F. Gatta, and S. Celozzi, "Hybrid and pi-circuit approaches for grounding system lightning response," in *2015 IEEE Eindhoven PowerTech, PowerTech 2015*, 2015.
- [9] S. Visacro and A. Soares, "HEM: A model for simulation of lightning-related engineering problems," *IEEE Transactions on Power Delivery*, vol. 20, no. 2 I, pp. 1206–1208, 2005.
- [10] S. A. Halin, A. H. A. Bakar, H. A. Illias, N. H. Hassan, H. Mokhlis, and V. Terzija, "Lightning backflashover tripping patterns on a 275/132 kV quadrupole circuit transmission line in Malaysia," *IET Science, Measurement & Technology*, vol. 10, no. 4, pp. 344 – 354, 2016.
- [11] IEEE, "Ieee recommended practice for determining the electric power station ground potential rise and induced voltage from a power fault," *IEEE Std 367-2012 (Revision of IEEE Std 367-1996)*, pp. 1–168, May 2012.
- [12] S. Bourg, B. Sacepe, and T. Debu, "Deep earth electrodes in highly resistive ground: frequency behaviour," in *Proceedings of International Symposium on Electromagnetic Compatibility*, Aug 1995, pp. 584–589.
- [13] L. Grcev and M. Popov, "On high-frequency circuit equivalents of a vertical ground rod," *IEEE Transactions on Power Delivery*, 2005.
- [14] L. Grcev and S. Grceva, "On hf circuit models of horizontal ground-

- ing electrodes,” *IEEE Transactions on Electromagnetic Compatibility*, vol. 51, no. 3, pp. 873–875, Aug 2009.
- [15] R. Velazquez and D. Mukhedkar, “Analytical Modeling of Grounding Electrodes Transient Behavior,” *IEEE Power Engineering Review*, vol. PER-4, no. 6, pp. 43–44, 1984.
- [16] L. Yang, G. Wu, and X. Cao, “An optimized transmission line model of grounding electrodes under lightning currents,” *Science China Technological Sciences*, vol. 56, no. 2, pp. 335–341, Feb 2013. [Online]. Available: <https://doi.org/10.1007/s11431-012-5072-6>
- [17] C. M. de Seixas and S. Kurokawa, “Using circuit elements to represent the distributed parameters of a grounding system under lightning strokes,” *Electric Power Systems Research*, vol. 172, pp. 213 – 220, 2019. [Online]. Available: <http://www.sciencedirect.com/science/article/pii/S0378779619301051>
- [18] M. A. O. Schroeder, M. T. C. de Barros, A. C. Lima, M. M. Afonso, and R. A. Moura, “Evaluation of the impact of different frequency dependent soil models on lightning overvoltages,” *Electric Power Systems Research*, vol. 159, pp. 40–49, 2018.
- [19] B. Gustavsen and A. Semlyen, “Rational approximation of frequency domain responses by vector fitting,” *IEEE Transactions on Power Delivery*, vol. 14, no. 3, pp. 1052–1061, July 1999.
- [20] J. R. Marti, “Accurate modelling of frequency-dependent transmission lines in electromagnetic transient simulations,” *IEEE Transactions on Power Apparatus and Systems*, vol. PAS-101, no. 1, pp. 147–157, Jan 1982.